



Short communication

Multilayered films of cobalt oxyhydroxide nanowires/manganese oxide nanosheets for electrochemical capacitor

Huajun Zheng^{a,b}, Fengqiu Tang^b, Melvin Lim^c, Aniruddh Mukherji^b, Xiaoxia Yan^b, Lianzhou Wang^{b,*}, Gao Qing (Max) Lu^{b,*}

^a State Key Laboratory Breeding Base of Green Chemistry Synthesis Technology, Zhejiang University of Technology, Hangzhou 310014, PR China

^b ARC Centre of Excellence for Functional Nanomaterials, School of Chemical Engineering and AIBN, The University of Queensland, St Lucia, Brisbane, QLD 4072, Australia

^c Division of Environmental and Water Resources Engineering, School of Civil and Environmental Engineering, Nanyang Technological University, 639798, Singapore

ARTICLE INFO

Article history:

Received 24 March 2009

Received in revised form 31 July 2009

Accepted 3 August 2009

Available online 12 August 2009

Keywords:

Manganese oxide nanosheet
Cobalt oxyhydroxide nanowire
Potentiostatic deposition
Electrostatic self-assembly
Electrochemical capacitor

ABSTRACT

Multilayered films of cobalt oxyhydroxide nanowires (CoOOH_{NW}) and exfoliated manganese oxide nanosheet (MONS) are fabricated by potentiostatic deposition and electrostatic self-assembly on indium-tin oxide coated glass substrates. The morphology and chemical composition of these films are characterized by scanning electron microscopy (SEM) and X-ray photoelectron spectra (XPS) and the potential application as electrochemical supercapacitors are investigated using cyclic voltammetry and charge–discharge measurements. These ITO/CoOOH_{NW}/MONS multilayered film electrodes exhibit excellent electrochemical capacitance properties, including high specific capacitance (507 F g⁻¹) and long cycling durability (less 2% capacity loss after 5000 charge/discharge cycles). These characteristics indicate that these newly developed films may find important application for electrochemical capacitors.

Crown Copyright © 2009 Published by Elsevier B.V. All rights reserved.

1. Introduction

Transition-metal oxide based materials have been used as electrode materials of rechargeable batteries and electrochemical capacitors (ECs) for decades [1], ruthenium oxide is at present known for its favorable pseudo-capacitive effects and very high specific capacitance (SC) but as well as its expensiveness. Other oxides of transition metals, such as manganese [2], cobalt [3], nickel [4] and tin [5] are currently the most promising candidates to replace ruthenium oxide as electrode materials for use in pseudo-capacitors, due to their low cost and no-toxicity. Toupin et al. [6] predicted a high SC of 1370 F g⁻¹ for MnO₂-based super-capacitor electrodes; however, practically, these oxides generally show values of merely one-sixth to one-fifth of the predicted value because dense MnO₂-based materials which possess low surface areas generally exhibit poor electronic conductivity and low electrochemical activity. On the other hand, it has also been reported that Co-based materials have good electrochemical activity but very narrow potential windows [7].

In attempting to boost ECs, much effort has focused on the development of bi- or tri-metal composites materials. For example,

nanostructured, microporous nickel-manganese oxide and cobalt-manganese oxide were deposited onto inexpensive stainless steel substrate by the potentiodynamic method [8]. Li et al. [9] reported the use of combined chemical and thermal methods to synthesize cobalt-manganese oxide materials. Their work indicate that new nanostructured composites can effectively enhance the electrochemical capacitance of transition-metal oxides, and thus offer new opportunities in using such newly developed materials for super-capacitor applications.

It is known that the structures and physical-chemical characteristics of composite metal oxides are strongly depended upon their preparative methods/conditions [10]. Generally, metal oxide materials developed by different methods exhibit different performances. In this work, we demonstrate a simple strategy in rationally designing a new type of multilayered films consisting exfoliated MnO₂ nanosheet (MONS) and cobalt oxyhydroxide nanowire (CoOOH_{NW}). The resulting multilayered films exhibited significantly improved electrochemical performance for pseudo-capacitors.

2. Experimental

2.1. Preparation of multilayered films of MONS and CoOOH_{NW}

The exfoliation of a layered compound of K_{0.45}MnO₂ was conducted as previously reported [11,12]. Briefly, the exfoliation of

* Corresponding authors. Tel.: +61 7 33463828; fax: +61 7 33656074.

E-mail addresses: l.wang@uq.edu.au (L. Wang), maxlu@uq.edu.au (G.Q. (Max) Lu).

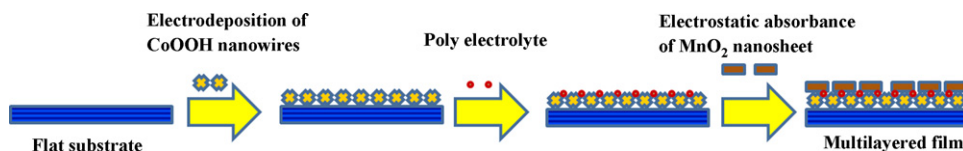


Fig. 1. Schematic illustration of preparation of the multilayered films.

a layered manganese oxide in a colloidal suspension containing well-dispersed MONS.

Multilayered films of MONS and CoOOHNW were prepared on a cleaned indium-tin oxide coated glass substrate (ITO substrate) via a two-step procedure as shown in Fig. 1. Firstly, a network of CoOOHNWs was prepared via electrodeposition on an ITO substrate from a solution of 0.05 M CoCl_2 operated at a potential of -0.95 V vs. Ag/AgCl [13]. The electrodeposition process was carried out in a three-electrode electrochemical cell in which the counter, reference, and working electrodes were a platinum (Pt) sheet, an Ag/AgCl electrode and an ITO glass slide, respectively. After the electrodeposition of the CoOOHNW layer, the sample was dipped in a poly(diallyldimethylammonium chloride) (PDDA) (1 wt.%, pH \approx 11) aqueous solution for 15 min and then rinsed thoroughly with water and dried with N_2 gas flow [11,12,14]. Then the PDDA-treated sample was subsequently placed horizontally into a well-dispersed of MONS (0.8 mg dm^{-3}) for 30 min, rinsed with water and dried with nitrogen gas flow to deposit MONS layer on the CoOOHNW layer. These subsequent three steps produce nanostructured composite films composed of (CoOOHNW/MONS) layers.

2.2. Film characterizations and electrochemical measurements

JEOL-6400 scanning electron microscopy (SEM) was used to examine the topographical features of the films prepared on the

ITO substrate. X-ray photoelectron spectra (XPS) data was acquired using a Kratos Axis Ultra X-ray photoelectron spectrometer and subsequently analyzed using CasaXPS software. The mass of each layer (PDDA/MONS or CoOOHNW) were obtained using the electrochemical quartz crystal microbalance (EQCM) technique, which have just been reported in our previous papers [11,12].

The electrochemical properties of the multilayered film electrodes were characterized by cyclic voltammetry (CV) and galvanostatic charge–discharge (GC) experiments in a standard three-electrode cell configuration with 0.1 M Na_2SO_4 solution as electrolyte. Multilayered film electrodes were dried at 120°C under vacuum for 3 h prior to electrochemical measurements in order to remove H_2O molecules from the films. A Pt sheet and an Ag/AgCl electrode served as the counter and reference electrodes. All CV and GC tests were performed using a Solartron Instrument Model 1480A multistat electrochemical interface and 1255B frequency response analyzer.

3. Results and discussion

Fig. 2 presents the SEM images of the multilayered films on ITO substrate. Fig. 2(A) shows the surface morphology of films by electrodeposition at a potential of -0.95 V from an electrolyte solution of 0.05 M CoCl_2 for 60 min. An irregularly distributed network of interconnected nanowires is observed to be packed on the surface.

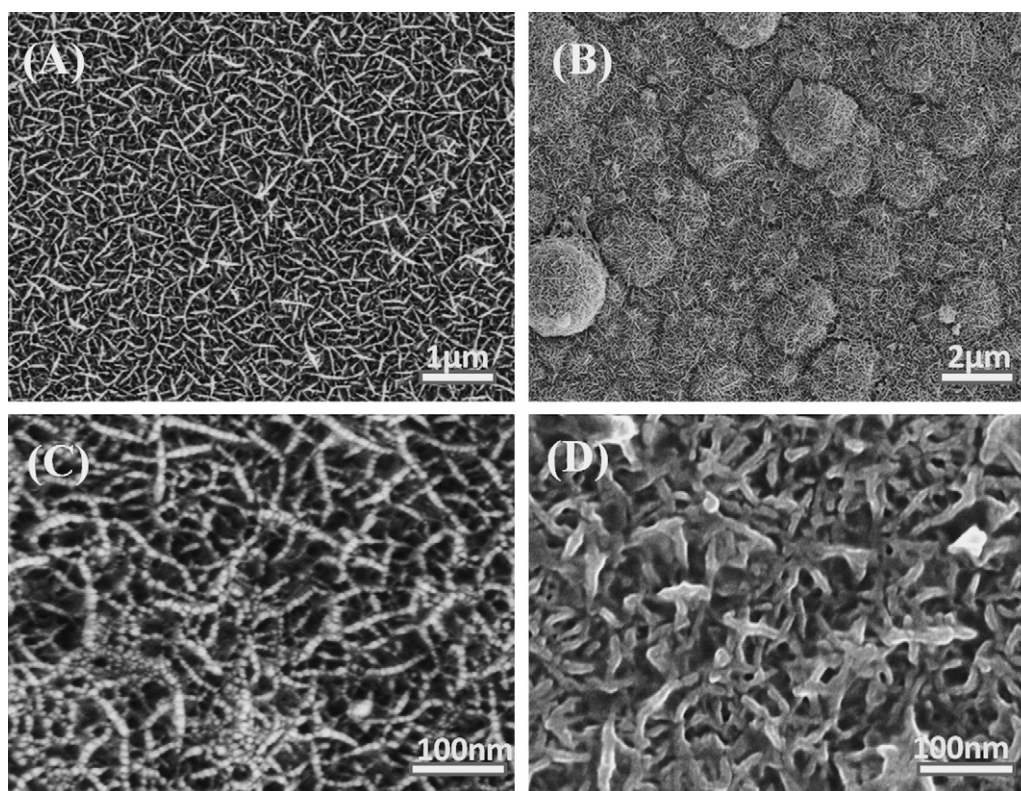


Fig. 2. SEM images of multilayered films deposited on ITO glass substrate. (A and C) Electrodeposition at a potential of -0.95 V from an electrolyte solution of 0.05 M CoCl_2 for 60 min, (B) electrodeposition at a potential of -0.95 V from an electrolyte solution of 0.05 M CoCl_2 for 120 min and (D) electrostatic deposition of exfoliated MnO_2 nanosheets on the surface of CoOOHNW layers.

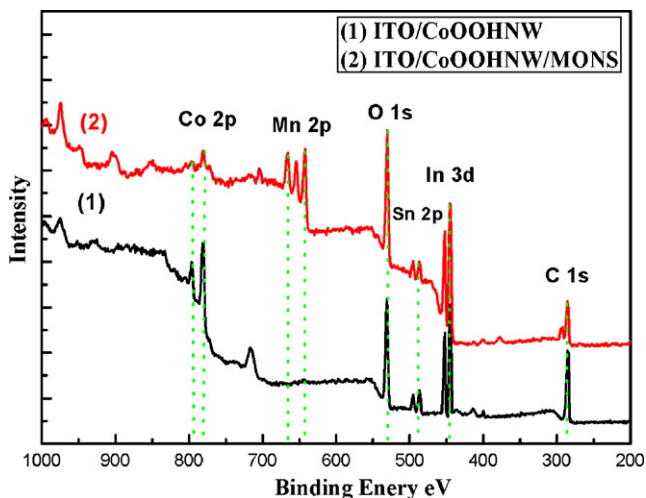


Fig. 3. XPS Spectrum for the multilayered films of (1) ITO/CoOOH/NW and (2) ITO/CoOOH/NW/MONS.

A deposition time of 60 min led to the substrate being uniformly covered with nanowires, whereas further increase of the deposition time caused the occurrence of spherical agglomerates on the deposited layer. Fig. 2(B) presents the morphology of film with its deposition time of 120 min. From high-magnification image (Fig. 2(C)), it is observed that the deposited layer is a networked microporous structure consisting of interconnected nanowires. The individual nanowire is linked by many nanodots into the size of a hundred of nanometers in length and of around 10 nm in thickness. Fig. 2(D) shows the surface of the multilayered film covered with a MONS layer on the CoOOH/NW layer. The networked structure of interconnected nanowires was still observed whereas the surfaces became rougher and larger because of the presence of a layer of MONS on the outer surface by electrostatic deposition of (PDDA/MONS).

XPS data provides evidence for presence of CoOOH or MnO₂ in different multilayered films. The XPS spectrum (Fig. 3) of the ITO/CoOOH/NW film shows the main peaks in the regions of Co (2p), In (3d), Sn (2p), and O (1s). Peaks that are assigned to In (3d), Sn (2p) and O (1s) were recorded at a binding energy of 445.1, 486.0 and 525.7 eV, indicating the presence of In₂O₃ and SnO₂ from ITO substrates. A well-resolved asymmetric peak at around 780.0 eV is observed in XPS spectra. In a separate study, Casella and Guascito [14] assigned this peak to the cobalt oxyhydroxide (CoOOH) species. The Co (2p_{3/2}) peak is also observed in the XPS spectrum of the ITO/CoOOH/NW/MONS multilayered film, but the intensity of peak is weaker compared with the ITO/CoOOH/NW film, possibly due to the presence of the MONS on the surface of the CoOOH layer. In addition, from spectrum 2, a series of peaks assigned to Mn (2p_{1/2}) and Mn (2p_{3/2}), are also recorded at a binding energy of 642.5 and 653.6 eV, respectively. This strongly indicates the successful electrostatic assembly of MONS on the CoOOH layer. On the other hand, a symmetrical peak of C (1s) centered at 284.7 eV in both the XPS spectrum of the ITO/CoOOH/NW and the ITO/CoOOH/NW/MONS multilayered film, is known as the characteristic signal raised from C=O bonds. These C=O bonds may be from acetone which is used during cleaning ITO substrate.

The electrochemical behavior of these multilayered film electrodes were investigated by CVs at a scan rate of 10 mV s⁻¹ in 0.1 M Na₂SO₄ aqueous solutions (Fig. 4). The CV curve of ITO/MONS electrode (curve 1) showed a typical pseudo-capacitive behavior in the potential range of 0.1–0.9 V. From this curve, it is observed that a broad peak around 0.76 V on the positive sweep and a peak centre at 0.60 V on the negative sweep are present, indicating the pseudo-

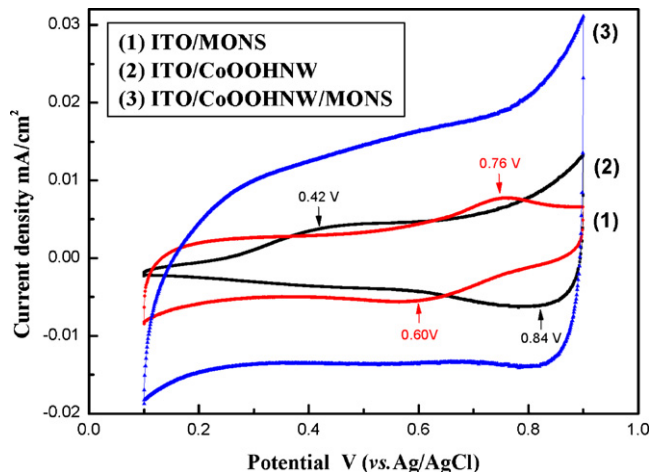


Fig. 4. CVs of various multilayered film electrodes in 0.1 M Na₂SO₄ electrolyte at scan rate of 10 mV/s. (1) ITO/MONS; (2) ITO/CoOOH/NW; (3) ITO/CoOOH/NW/MONS.

capacitance from the Mn⁴⁺/Mn³⁺ reversible redox process. This broad peak appears on the positive sweep due to the reversible insertion/extraction of a Na⁺ or H⁺ present in the electrolyte [6]. Similarly, for the ITO/CoOOH/NW electrode, a broad peak around 0.42 V on the positive sweep and a peak centre at 0.84 V on the negative sweep are present, also indicating pseudo-capacitance. It can

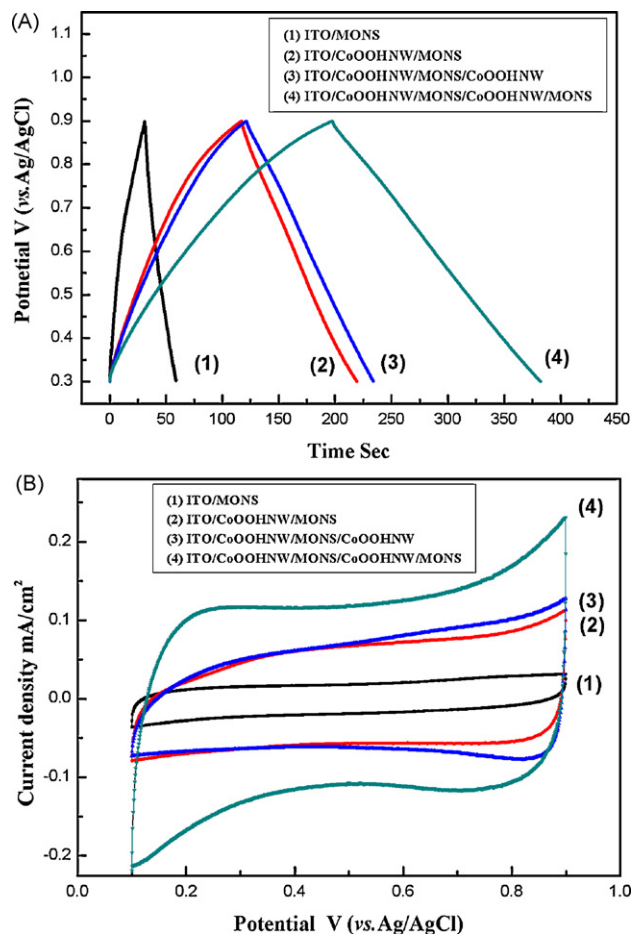


Fig. 5. Chronopotentiograms of various multilayered film electrodes at charge-discharge current density of $1 \times 10^{-5} \text{ Acm}^{-2}$ (A) and CVs of various multilayered film electrodes in 0.1 M Na₂SO₄ electrolyte at scan rate of 50 mV/s (B). (1) ITO/MONS; (2) ITO/CoOOH/NW/MONS; (3) ITO/CoOOH/NW/MONS/CoOOH/NW; (4) ITO/CoOOH/NW/MONS/CoOOH/NW/MONS.

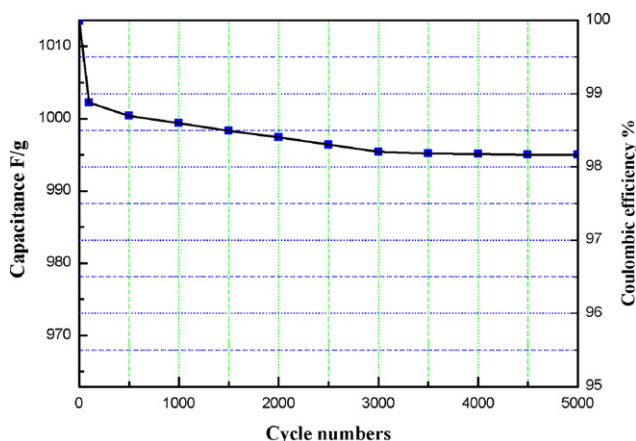


Fig. 6. Dependence of capacitance and coulombic efficiency on cycling number. (ITO/CoOOH/NW/MONS electrode in 0.1 M Na₂SO₄ electrolyte, measurement current of 0.1 mA).

be seen clearly that this electrode shows a limited potential window in the range of 0.3–0.9 V. As seen in the CV of ITO/CoOOH/NW/MONS film, the capacitive current is relatively larger compared with both the ITO/MONS and ITO/CoOOH/NW electrode. Furthermore, the potential window, with a nearly ideal rectangular profile in the range of 0.1–0.9 V, has clearly become significantly larger than that presented by the ITO/CoOOH/NW electrode.

It is clear that the CoOOH/NW layer play an important role in the electrochemical performance of multilayered films by contrast to the SC values of multilayered film electrodes. Fig. 5(A) presents the chronopotentiograms of these four types of multilayered film electrodes at charge–discharge current density of $1 \times 10^{-5} \text{ A cm}^{-2}$ in 0.1 M Na₂SO₄ electrolyte. Based on the results of the EQCM method and the experimental results shown in Fig. 5(A), the mass of PDDA/MONS and CoOOH/NW layer are 2.75×10^{-6} and 2.27×10^{-6} g, and the single-electrode specific capacitances of ITO/MONS, ITO/CoOOH/NW/MONS, ITO/CoOOH/NW/MONS/CoOOH/NW and ITO/(CoOOH/NW/MONS)₂ electrode are 252, 507, 523 and 856 F g⁻¹, respectively. By contrast with the SC values of ITO/MONS and ITO/CoOOH/NW/MONS, it is observed that the differences in the values hint on the importance of the COH/NW layer in the multilayered film. On the other hand, the comparison of the SC values between ITO/CoOOH/NW/MONS and ITO/CoOOH/NW/MONS/CoOOH/NW multilayered film electrodes shows that there is only a slight increase in capacitance increase with adding a layer of CoOOH/NW on the surface of the multi-layered film electrodes. This observation is further confirmed by CV measurements shown in Fig. 5(B). The box areas of the CVs are similar, but the redox reaction peaks of different metals appear in different regions. Generally, anodic peaks and cathodic peaks in the neutral electrolyte are attributed to the quasi-reversible Co(OH)₂/CoOOH and CoOOH/CoO₂ redox process [7]. Curve 2 in Fig. 5(B) shows that the peaks from the pseudo-capacitive behavior of cobalt are weak. Moreover, compared with curves 2 and 3, we observe that the manganese redox peaks which appear around 0.76 V (vs. Ag/AgCl) are also restricted because the COH/NW layer covered the outer surface of MONS layer. Similar conclusion was obtained in another important aspect of the ITO/(MONS/CoOOH/NW)₂ multilayered film electrode. From curve 4 in Fig. 5(B), the box area of CV curve of ITO/(MONS/CoOOH/NW)₂ electrode is much larger than ITO/MONS/CoOOH/NW electrode. Also, as previously described,

the SC of ITO/(MONS/CoOOH/NW)₂ electrode is up to 856 F g⁻¹, relatively larger than the ITO/CoOOH/NW/MONS/CoOOH/NW electrode. It can be explained that the CoOOH/NW layer contributes significantly to the enhanced capacitance of composite electrode by mainly providing a networked microporous structure with a large surface and an effective path for the electrochemical process, by merely its redox process. In other word, it is likely that the effect of CoOOH/NW layer may be accounted for full utilization of the electroactive MONS outer layer loading on the CoOOH/NW nanostructure network.

The electrochemical stability of the ITO/CoOOH/NW/MONS multilayered film electrode was examined by charge–discharge cycling in 0.1 M Na₂SO₄ electrolyte at a current of 0.1 mA, as shown in Fig. 6. A small decrease in SC after the initial 100 cycles was observed, but the capacity loss after 5000 consecutive cycles is a mere 1.87%. This indicates that the ITO/CoOOH/NW/MONS multilayered film electrode can behave reversibly as an excellent capacitor material for a large number of charge–discharge cycles.

4. Conclusions

Multilayered film electrodes for electrochemical capacitors, containing transition-metal composite materials, were successfully fabricated by alternately potentiostatic deposition of CoOOH/NW and electrostatic assembly of MONS. The multilayered film electrodes exhibited excellent electrochemical capacitance and very long cycling durability. Electrochemical studies on the electrodes indicate that the CoOOH/NW layer is a key point in offering the excellent electrochemical activity in the multilayered films, as it provides a large surface area for the dispersion of MONS. The optimized deposition sequence of CoOOH/NW and MONS in the multilayered films led to apparently enhanced electrochemical capacity. This indicates that rational design in these newly developed multilayered film electrodes could lead to the development of important electrodes for highly efficient electrochemical capacitors.

Acknowledgements

This work was financially supported by the Zhejiang Natural Science Foundation (No. Y4080042) and the Australian Research Council under its Centres of Excellence and DP Programs. Huajun Zheng is grateful for the financial support from China Scholarship Council (CSC).

References

- [1] B.E. Conway, V. Birss, J. Wojtowicz, *J. Power Sources* 66 (1997) 1.
- [2] K.R. Prasad, N. Miura, *J. Power Sources* 135 (2004) 354.
- [3] E. Hosono, S. Fujihara, I. Honma, M. Ichihara, H. Zhou, *J. Power Sources* 158 (2006) 779.
- [4] Y. Wang, Y. Xia, *Electrochim. Acta* 51 (2006) 3223.
- [5] K.R. Prasad, N. Miura, *Electrochem. Commun.* 6 (2004) 849.
- [6] M. Toupin, T. Brousse, D. Bélanger, *Chem. Mater.* 16 (2004) 3184.
- [7] P.K. Nayak, N. Munichandraiah, *J. Electrochem. Soc.* 155 (2008) A855.
- [8] K.R. Prasad, N. Miura, *Electrochem. Commun.* 6 (2004) 1004.
- [9] Q. Li, K.-x. Li, J.-y. Gu, H. Fan, *J. Phys. Chem. Solids* 69 (2008) 1733.
- [10] E. Vila, R.M. Rojas, J.L. Martín de Vidales, O.G. Martínez, *Chem. Mater.* 8 (1996) 1078.
- [11] H. Zheng, F. Tang, Y. Jia, L. Wang, Y. Chen, M. Lim, L. Zhang, G. Max Lu, *Carbon* 47 (2009) 1534.
- [12] H. Zheng, F. Tang, M. Lim, T. Rufford, A. Mukherji, L. Wang, G. Max Lu, *J. Power Sources* 193 (2009) 930.
- [13] Q. Nguyen, L. Wang, G. (Max) Lu, *Int. J. Nanotechnol.* 4 (2007) 585.
- [14] I.G. Casella, M.R. Guascito, *J. Electroanal. Chem.* 476 (1999) 54.